Organic & Biomolecular Chemistry

PAPER

View Article Online
View Journal | View Issue

Cite this: *Org. Biomol. Chem.*, 2017, **15**, 2797

Rapidly accessible "click" rotaxanes utilizing a single amide hydrogen bond templating motif†

Beth E. Fletcher, Michael J. G. Peach and Nicholas H. Evans*

Received 6th February 2017,
Accepted 6th March 2017

DOI: 10.1039/c7ob00284j

rsc.li/obc

The synthesis of hydrogen bond templated rotaxanes using the CuAAC click reaction has been achieved in yields of up to 47%, employing near stoichiometric equivalents of macrocycle and readily prepared azide and alkyne half-axle components. Interlocked structure formation has been confirmed by NMR spectroscopy and mass spectrometry. Density functional theory calculations support ^{1}H NMR spectroscopic analysis that the macrocycle resides over the amide of the axle component, rather than the newly formed triazole, as a result of more favourable hydrogen bond interactions.

Introduction

Rotaxanes,[1] interlocked molecules consisting of macrocyclic ring(s) trapped on stoppered axle(s), have been applied to a number of nanotechnological applications,[2] some of which rely on the relative motion of their ring and axle components.[3] Alongside metal cations[4] and π–π donor–acceptor interactions,[5] hydrogen bonding,[6] sometimes augmented with additional cationic[7] or anionic[8] assistance, has proven a popular choice of template to generate rotaxanes. While a large number of protocols for rotaxane synthesis have now been disclosed, new synthetic routes that allow rapid access to rotaxanes in good yield and using only stoichiometric amounts of precursor components – that minimises waste – are still of considerable interest.

Little used to date has been an elegantly simple hydrogen bond templation system reported by Philp and co-workers in 2008.[9] This relies upon the hydrogen bond templated threading of an amide containing component through a 2,6-bis-amide pyridyl macrocycle, followed by covalent capture of the resulting pseudo-rotaxane by either maleimide/nitrone 1,3-dipolar cycloaddition[9–11] or aza-Wittig reaction.[12]

Inspired by this work, we chose to investigate and are able to report the isolation of rotaxanes in good yields by use of the straightforward and versatile CuAAC click reaction[13] to stopper an azide half-axle, that contains the critical amide functional group required for the pre-requisite pseudo-rotaxane formation with a polyether-isophthalamide macrocycle (Fig. 1). Interlocked structure formation was confirmed by ^{1}H NMR spectroscopy and mass spectrometry. Density functional theory calculations support ^{1}H NMR spectroscopic analysis which suggests that in the prepared rotaxanes the macrocyclic ring remains over the amide of the axle component rather than translating to the newly formed triazole.

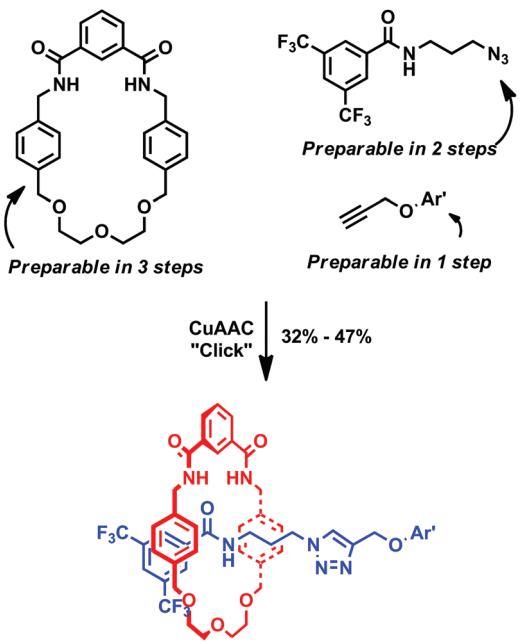

Fig. 1 Schematic representation of the rapid synthesis of rotaxanes utilizing a single amide hydrogen bond templating motif and the CuAAC click reaction.

Results and discussion

Synthesis of rotaxane precursors

The structures of all rotaxane precursors used in this study, along with the syntheses of novel compounds, are presented in

Department of Chemistry, Lancaster University, Lancaster, LA1 4YB, UK.
E-mail: n.h.evans@lancaster.ac.uk

†Electronic supplementary information (ESI) available: Additional notes on experimental procedures; copies of characterisation spectra of novel compounds and further computational modelling data. See DOI: 10.1039/c7ob00284j

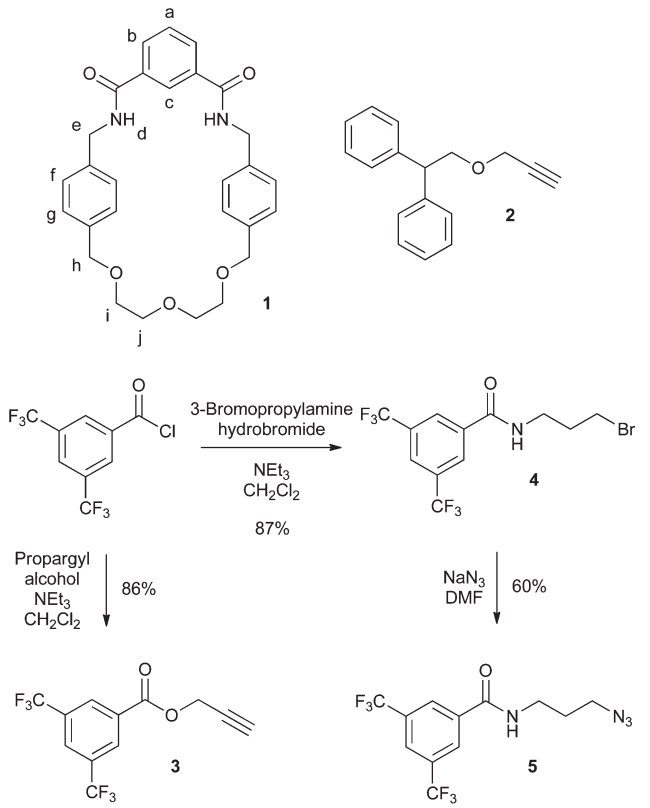

Scheme 1 Structures of rotaxane precursors and syntheses of novel intermediates and precursors used in this study.

Scheme 1. Previously reported macrocycle **1** [14] has now been prepared in higher yield by use of a template method (see ESI†), while diphenyl alkyne **2** [15] was prepared according to the previously reported procedure. Novel alkyne stopper **3** was prepared by simply reacting equimolar amounts of 3,5-bis(trifluoromethyl)benzoyl chloride and propargyl alcohol, with excess NEt_3 in dry CH_2Cl_2. After aqueous workup, **3** was isolated in 86% yield. The azide click precursor was prepared in two steps. First bromo-amide **4** was prepared by reacting equimolar amounts of 3,5-bis(trifluoromethyl)benzoyl chloride and 3-bromopropylamine hydrobromide, with excess NEt_3 in dry CH_2Cl_2. After aqueous workup, **4** was isolated in 87% yield. Conversion to azide **5** was accomplished by heating a solution of **4** in dry DMF with excess NaN_3 at 80 °C. After dilution, and extraction, **5** was isolated in 60% yield. The successful preparation of novel compounds **3–5** was confirmed by NMR and IR spectroscopies and mass spectrometry (see ESI†).

"Click" synthesis and spectral characterisation of rotaxanes

Synthesis of rotaxanes **6** and **7** were attempted as according to Scheme 2. In each case, to a solution of macrocycle **1** in dichloromethane, 1.1 equivalents of azide **5** and 1.1 equivalents of alkyne (**2** or **3**) were added. These were followed by catalytic $Cu(CH_3CN)_4BF_4$ and TBTA, and 1.2 equivalents of DIPEA. The reactions were stirred overnight at room temperature under an inert atmosphere, and then submitted to aqueous workup, before purification on silica. By analogous reactions (in the absence of macrocycle **1**), non-interlocked axles **8** and **9** were

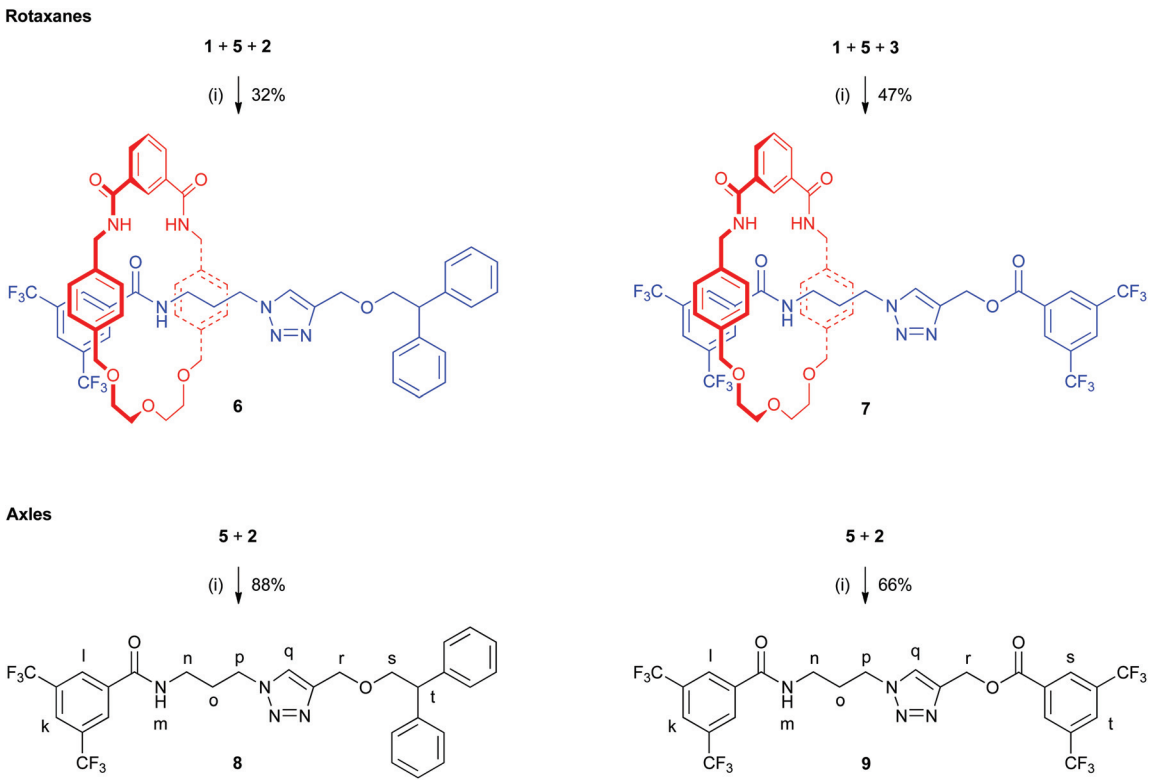

Scheme 2 Syntheses of rotaxanes **6** and **7** and non-interlocked axles **8** and **9**. Reaction conditions: (i) cat. $Cu(CH_3CN)_4BF_4$, cat. TBTA, DIPEA, CH_2Cl_2.

also prepared (in 88% and 66% yield respectively) to aid ^{1}H NMR spectroscopic interpretation.

It was not possible to separate rotaxane **6** and unthreaded macrocycle **1** by silica gel column chromatography. Purification using prep TLC, allowed for isolation of pure rotaxane **6** in a reasonable 32% yield. Pleasingly, rotaxane **7** could be purified by careful column chromatography, being isolated in a yield of 47%.

The ^{1}H NMR spectrum of rotaxane **6**, along with that of non-interlocked macrocycle **1** and axle **8** for comparison, is shown in Fig. 2.[16] The upfield shift and splitting of protons *f* and *g* in rotaxane **6** compared to macrocycle **1** is consistent with intercalation of the axle component between the aromatic rings of the macrocycle. The downfield shift of protons *c* and *d* in the rotaxane are indicative of interactions with a hydrogen bond acceptor on the axle. The functional group of the axle residing within the macrocyclic ring in rotaxane **6** is believed to be the templating amide, and not the newly formed triazole. Evidence for this conclusion is provided by the large upfield shifts in axle protons *m* and *n* and in particular the lack of a significant shift in proton *r*. Another notable feature of the ^{1}H NMR spectrum of rotaxane **6** is the splitting of protons *e*, *h*, *i* and *j*, which arise from the two faces of the macrocycle no longer being equivalent in the rotaxane due to the directionality of the threaded axle. Comparison of the ^{1}H NMR spectra of macrocycle **1**, rotaxane **7** and axle **9** reveals similar trends, indicative of the macrocycle also residing over the axle amide in rotaxane **7**, rather than the triazole or ester (see ESI†).[16]

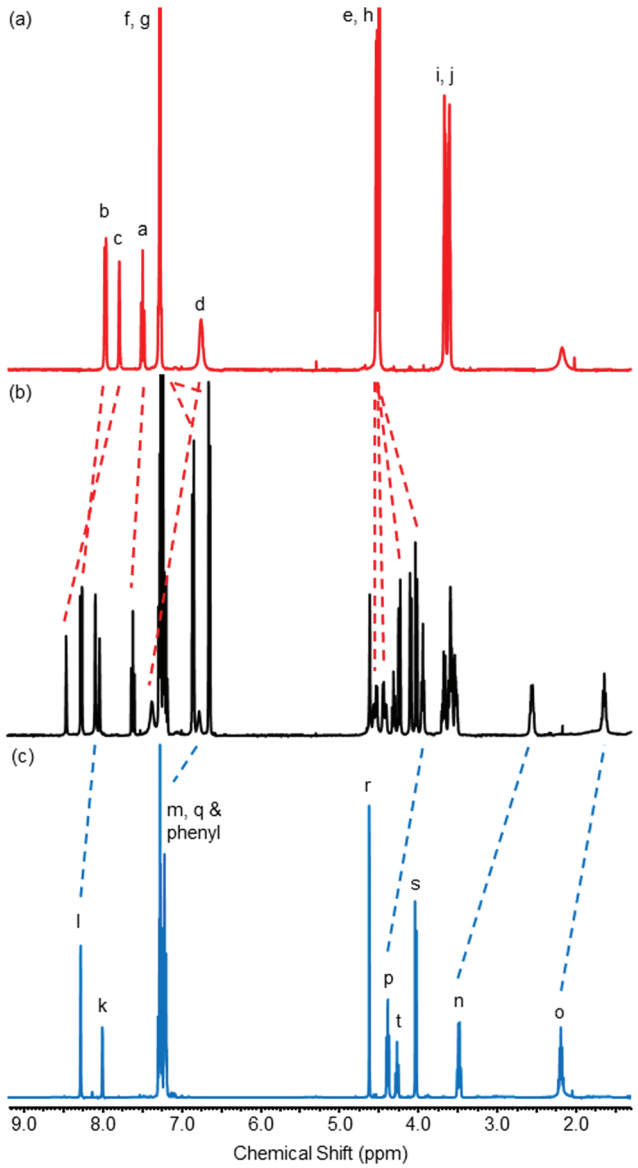

Fig. 2 ^{1}H NMR spectra of (a) macrocycle **1**, (b) rotaxane **6** and (c) axle **8** ($CDCl_3$, 400 MHz, 298 K). For atom labels see Schemes 1 and 2.

The interlocked natures of rotaxanes **6** and **7** are further supported by the appearance of through-space correlations being observed in the ^{1}H–^{1}H ROESY NMR spectra between signals arising from protons in the macrocyclic and axle components (see ESI†). In addition, molecular ion peaks for the rotaxanes are observed in the positive-ion electrospray mass spectra (see ESI†).

Computational modelling of rotaxanes

While reasonably confident in our deduction that the macrocycle is residing over the axle amide, and not the triazole functionality, in both rotaxanes, we sought further evidence to confirm the co-conformational behaviour of the rotaxanes. Unable to grow single crystals for X-ray structure determination, we therefore turned our attention to computational modelling. Density-functional theory (DFT) calculations were undertaken on both **6** and **7**.[17] The calculations were performed using the Gaussian 09 program,[18] using the B3LYP exchange–correlation functional[19] together with the 6-31G* basis set for all atoms. Solvent effects ($CHCl_3$) were modelled using a polarisable continuum model, using the default solvent cavity parameters as defined in Gaussian 09.

For each of the rotaxanes, geometry optimisations were run with the macrocycle starting over (i) the amide and (ii) the triazole functional groups of the axle component.[20] Distinct optimised structures were obtained in each case (see Fig. 3 and ESI†), but for both rotaxanes there was an energetic preference for the macrocycle being over the amide "station" (41 kJ mol^{-1} for **6** and 76 kJ mol^{-1} for **7**).[21]

Inspection of the optimised structures suggests that this preference is due to more favourable hydrogen bonding interactions being present when the amide "station" is occupied by the macrocycle.[21] In this case the isophthalamide of the macrocycle adopts a *syn–syn* conformation and presents three hydrogen bond donors to the O atom of the amide "station". If the macrocycle resides at the triazole "station", the isophthalamide adopts a *syn–anti* conformation, resulting in only one N–H hydrogen bond donating to the N atom of the triazole.[22] Also, in the preferred amide "station" co-conformation, the triazole C–H hydrogen bonds to a polyether oxygen on the macrocyclic ring, further stabilising this conformation. A structural consequence of this additional hydrogen bonding interaction is to bend the axle, such that protons *o* and *p* are

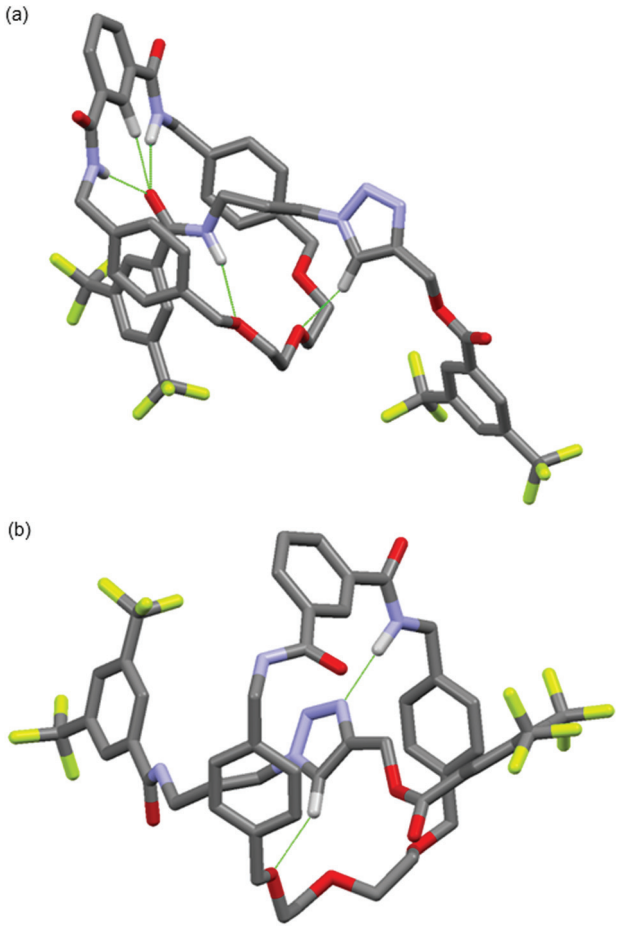

Fig. 3 Minimum energy structures of rotaxane **7** with macrocycle occupying (a) amide and (b) triazole "stations". Hydrogen bonds are represented by green dashed lines. Hydrogen atoms not participating in hydrogen bonding are omitted for clarity.

partially within the macrocycle cavity, which is consistent with the significant upfield shifts of these protons in the rotaxane ^{1}H NMR spectra compared to the spectra of the free axles (see Fig. 2 and ESI†). Finally, there is a substantially greater difference in energies for the two co-conformations of rotaxane **7** (compared to **6**). We attribute this to the disruption in the planarity of the ester and bulky aromatic stopper group in the co-conformation of **7** when the macrocycle occupies the neighbouring triazole "station" (Fig. 3b).

Conclusions

This study has demonstrated it is possible to generate rotaxanes by short, straightforward and highly yielding reaction sequences, employing CuAAC click chemistry to stopper Philp-style self-assembled pseudo-rotaxanes of an amide half-axle threaded through an aryl bis-amide macrocycle. Density functional theory calculations provide strong supporting evidence for the co-conformational behaviour of the prepared rotaxanes, with the macrocycle remaining over the templating amide of the axle, rather than over the newly formed triazole functionality.

We are confident that the synthetic ease in generating these rotaxanes will not only be appealing to those already preparing rotaxanes, but will encourage other chemists to begin using rotaxanes in their own research. We ourselves are undertaking further study of this class of rotaxane with respect to synthetic methodology development and molecular motion and host–guest applications.

Experimental

General information

Commercially available solvents and chemicals were used without further purification unless stated. Dry solvents, NEt_3 and DIPEA were purchased dry and stored under an inert atmosphere. $Cu(CH_3CN)_4BF_4$ was stored in a desiccator over P_4O_{10}. Deionised water was used in all cases. Previously reported macrocycle **1** [14] has now been prepared in higher yield by use of a template method, details of which may be found in the ESI.† Alkyne **2** was prepared as according to the previously reported procedure.[15]

Silica gel with a 60 Å particle size was used as the stationary phase for column chromatography. Analytical TLC was used to monitor the progress of column chromatography and analytical TLC plates were typically examined under short wavelength (λ = 254 nm) UV light. If required, ceric ammonium molybdate or potassium permanganate stains were used to develop the analytical TLC plates. Preparatory TLC was carried out on silica gel possessing a fluorescent indicator to allow for examination with short wavelength UV light.

IR spectra were recorded on an Agilent Technologies Cary 630 FTIR spectrometer. NMR spectra were recorded on a Bruker Ultrashield 400 Plus spectrometer at 298 K, with the NMR data reported below assigned according to the atom labels to be found in the Schemes 1 and 2. Mass spectra were recorded on a Waters Xevo G2-S or Thermofisher LTQ Orbitrap XL at the EPSRC UK National Mass Spectrometry Facility at Swansea University, UK, or a Shimadzu LCMS IT ToF instrument at Lancaster University, UK. Melting points were recorded on a Gallenkamp capillary melting point apparatus and are uncorrected.

Experimental procedures

Alkyne 3. 3,5-Bis(trifluoromethyl)benzoyl chloride (491 μL, 750 mg, 2.71 mmol) dissolved in dry CH_2Cl_2 (10 mL) was added dropwise to a solution of propargyl alcohol (160 μL, 151 mg, 2.71 mmol) and NEt_3 (944 μL, 686 mg, 6.78 mmol) dissolved in dry CH_2Cl_2 (20 mL) at 0 °C under an Ar (g) atmosphere. The ice bath was removed and the reaction was stirred for 1 h, maintaining the Ar (g) atmosphere. The reaction mixture was then washed with 10% HCl (aq) (2 × 25 mL) and 10% Na_2CO_3 (aq) (2 × 25 mL). The organic layer was separated, dried ($MgSO_4$), filtered and solvent removed *in vacuo* to yield the title compound as a very pale yellow oil (690 mg, 86%).

ν_{max}/cm^{-1} (neat) 3310 (C–H), 1740 (C═O), 1360, 1280, 1240, 1180, 1130. δ_H(400 MHz; $CDCl_3$) 8.53 (2H, s, Ar*H*), 8.10 (1H, s, Ar*H*), 5.01 (2H, d, ^4J = 2.5 Hz, CH_2), 2.59 (1H, t, ^4J = 2.5 Hz, CH_2). δ_C(100 MHz; $CDCl_3$) 163.2 (C═O), 132.3 (quar, ^2J = 34 Hz, $ArCCF_3$), 131.6 (ArC), 129.9 (ArC), 126.7 (ArC), 122.8 (quar, ^1J = 288 Hz, CF_3), 75.9 (CH), 53.5 (OCH_2). δ_F(377 MHz; $CDCl_3$) −63.0. *m*/*z* (ASAP) 296.0277 ($[M]^+$ $C_{12}F_6H_6O_2$ requires 296.0272).

Bromo-amide 4. 3,5-Bis(trifluoromethyl)benzoyl chloride (491 μL, 750 mg, 2.71 mmol) dissolved in dry CH_2Cl_2 (10 mL) was added dropwise to a solution of 3-bromopropylamine hydrobromide (593 mg, 2.71 mmol) and NEt_3 (944 μL, 686 mg, 6.78 mmol) dissolved in dry CH_2Cl_2 (20 mL) at 0 °C under an Ar (g) atmosphere. The ice bath was removed and the reaction was stirred for 1 h, maintaining the Ar (g) atmosphere. The reaction mixture was then washed with 10% HCl (aq) (2 × 25 mL), 10% KOH (aq) (2 × 25 mL) and H_2O (1 × 25 mL). The organic layer was separated, dried ($MgSO_4$), filtered and solvent removed *in vacuo* to yield the title compound as a waxy white solid (893 mg, 87%). Mp 74–76 °C. ν_{max}/cm^{-1} (neat) 3280 (N–H), 3100 (C–H), 1650 (C═O), 1620, 1550, 1450, 1390, 1320, 1280, 1120. δ_H(400 MHz; $CDCl_3$) 8.23 (2H, s, Ar*H*), 8.01 (1H, s, Ar*H*), 6.70 (1H, br s, N*H*), 3.66–3.71 (2H, app quar, NHCH_2), 3.52 (2H, t, ^3J = 6.4 Hz, CH_2Br), 2.22–2.28 (2H, app quin, $NHCH_2CH_2$). δ_C(100 MHz; $CDCl_3$) 164.9 (C═O), 136.3 (ArC), 132.2 (quar, ^2J = 32 Hz, $ArCCF_3$), 127.3 (ArC), 125.1 (ArC), 122.8 (quar, ^1J = 271 Hz, CF_3), 39.2 ($NHCH_2$), 31.9 (CH_2Br), 30.7 (CH_2). δ_F(377 MHz; $CDCl_3$) −63.0. *m*/*z* (ES) 399.9741 ($[M + Na]^+$ $C_{12}F_6H_{10}NNaO$ requires 399.9742).

Azide 5. NaN_3 (650 mg, 11.1 mmol) was added to a solution of **4** (842 mg, 2.22 mmol) in dry DMF (20 mL) under an Ar (g) atmosphere. The reaction was heated to 80 °C with stirring for 24 h, maintaining the Ar (g) atmosphere. After cooling to RT, H_2O (125 mL) was added, then the resulting solution was extracted with CH_2Cl_2 (6 × 30 mL). The combined organic layers were dried ($MgSO_4$), filtered and concentrated to give a golden oil. To remove remaining DMF, the oil was re-dissolved in CH_2Cl_2 (20 mL) and washed with H_2O (3 × 100 mL). The organic layer was dried ($MgSO_4$), filtered and solvent removed *in vacuo* to yield the title compound as a pale golden oil (461 mg, 60%). ν_{max}/cm^{-1} (neat) 3300 (N–H), 3090 (C–H), 2940 (C–H), 2100 (N═N═N), 1650 (C═O), 1550, 1470, 1380, 1270, 1170, 1130. δ_H(400 MHz; $CDCl_3$) 8.23 (2H, s, Ar*H*), 8.02 (1H, s, Ar*H*), 6.61 (1H, br s, N*H*), 3.59–3.64 (2H, app quar, NHCH_2), 3.50 (2H, t, ^3J = 6.4 Hz, CH_2N_3), 1.92–1.99 (2H, app quin, $NHCH_2CH_2$). δ_C(100 MHz; $CDCl_3$) 164.7 (C═O), 136.4 (ArC), 132.2 (quar, ^2J = 34 Hz, $ArCCF_3$), 127.2 (ArC), 125.1 (ArC), 122.8 (quar, ^1J = 271 Hz, CF_3), 49.7 (CH_2N_3), 38.4 ($NHCH_2$), 28.5 (CH_2). δ_F(377 MHz; $CDCl_3$) −62.9. *m*/*z* (APC) 339.0680 ($[M - H]^-$ $C_{12}F_6H_9N_4O$ requires 339.0686).

Rotaxane 6. Macrocycle **1** (20 mg, 0.042 mmol) and azide **5** (16 mg, 0.046 mmol) were dissolved in dry CH_2Cl_2 (1 mL) under an Ar (g) atmosphere. Then alkyne **2** (12 mg, 0.046 mmol), $Cu(CH_3CN)_4BF_4$ (1.4 mg, 0.0046 mmol), TBTA (2.4 mg, 0.0046 mmol) and DIPEA (9 μL, 6.6 mg, 0.051 mmol) were added. The reaction was stirred at RT for 18 h under an Ar (g) atmosphere. Then, the reaction was diluted to 10 mL, washed with 0.02 M EDTA in 1 M NH_3 (aq) solution (2 × 10 mL) and (1 × 10 mL) brine. The organic layer was dried ($MgSO_4$), filtered and solvent removed *in vacuo*. The crude material was submitted to silica gel column chromatography (99 : 1 to 98 : 2 CH_2Cl_2/CH_3OH), which allowed for isolation of the product contaminated with macrocycle **1**. Pure rotaxane **6** was obtained by use of prep TLC (repeated running in 98 : 2 CH_2Cl_2/CH_3OH) to give the title compound as a transparent colourless film (14 mg, 32%). R_f = 0.20, 98 : 2 CH_2Cl_2/CH_3OH. ν_{max}/cm^{-1} (neat) 3320 (N–H), 3060 (C–H), 2920 (C–H), 2870 (C–H), 1650 (C═O), 1530, 1450, 1360, 1280, 1180, 1130, 1080. δ_H(400 MHz; $CDCl_3$) 8.47 (1H, s, H^c), 8.27 (2H, dd, ^3J = 7.8 Hz, ^4J = 1.6 Hz, H^b) 8.09 (2H, s, H^l), 8.04 (1H, s, H^k), 7.62 (1H, t, ^3J = 7.8 Hz, H^a), 7.39 (2H, br s, H^d), 7.18–7.30 (11H, m, H^q & phenyl *H*), 6.86 (4H, d, ^3J = 8.0 Hz, H^f), 6.78 (1H, br s, H^m), 6.65 (4H, d, ^3J = 8.0 Hz, H^g), 4.62 (2H, s, H^r), 4.52–4.57 (2H, m, H^e), 4.40–4.45 (2H, m, H^e), 4.31 (1H, t, ^3J = 7.2 Hz, H^t), 4.24 (2H, d, ^3J = 10.0 Hz, H^h), 4.10 (2H, d, ^3J = 7.2 Hz, H^s), 4.03 (2H, d, ^3J = 10.0 Hz, H^h), 3.95 (2H, t, ^3J = 6.8 Hz, H^p), 3.50–3.71 (8H, m, H^i & H^j), 2.55–2.59 (2H, app quar, H^n), 1.61–1.68 (2H, app quin, H^o). δ_C(100 MHz; $CDCl_3$) 166.6, 164.2 (2 × C═O), 141.8, 137.8, 136.0, 135.5, 134.1, 131.7, 131.3, 129.3, 128.7, 128.5, 128.4 128.2, 126.6, 124.6, 124.4, 123.6, 121.7, 74.2(C^s), 73.6 (C^h), 70.7, 69.6, 64.0 (C^r), 51.0 (C^t), 48.0 (C^p), 44.1 (C^e), 37.4 (C^n), 28.1 (C^o). δ_F(377 MHz; $CDCl_3$) −62.5. *m*/*z* (ES) 1073.4014 ($[M + Na]^+$ $C_{57}F_6H_{56}N_6NaO_7$ requires 1073.4007).

Rotaxane 7. An identical reaction to that for rotaxane **6** was carried out, except the substitution of alkyne **3** for alkyne **2**. After the aqueous workup, the crude material was purified by silica gel column chromatography (98 : 2 CH_2Cl_2/CH_3OH) to give the title compound as a transparent colourless film (22 mg, 47%). R_f = 0.17, 98 : 2 CH_2Cl_2/CH_3OH. ν_{max}/cm^{-1} (neat) 3330 (N–H), 3060 (C–H), 2920 (C–H), 2870 (C–H), 1730 (ester C═O), 1650 (amide C═O), 1520, 1460, 1380, 1360, 1280, 1240, 1170, 1130, 1080. δ_H(400 MHz; $CDCl_3$) 8.48 (2H, s, H^s), 8.45 (1H, s, H^c), 8.28 (2H, dd, ^3J = 7.8 Hz, ^4J = 1.6 Hz, H^b), 8.08 (2H, s, H^l), 8.05 (2H, app br s, H^k & H^t), 7.17 (1H, s, H^q), 7.64 (1H, t, ^3J = 7.8 Hz, H^a), 7.30 (2H, t, ^3J = 4.6 Hz, H^d), 6.87 (4H, d, ^3J = 8.1 Hz, H^f), 6.80 (1H, t, ^3J = 5.3 Hz, H^m), 6.65 (4H, d, ^3J = 8.1 Hz, H^g), 5.51 (2H, s, H^r), 4.61–4.66 (2H, m, H^e), 4.32–4.37 (2H, m, H^e), 4.28 (2H, d, ^3J = 9.6 Hz, H^h), 4.00–4.04 (4H, m, H^h & H^p), 3.54–3.77 (8H, m, H^i & H^j), 2.57–2.62 (2H, app quar, H^n), 1.65–1.73 (2H, app quin, H^o). δ_C(100 MHz; $CDCl_3$) 166.3, 164.1, 163.8 (3 × C═O), 141.3, 137.6, 136.1, 135.4, 134.0, 132.3 (quar, ^2J = 34 Hz, $ArCCF_3$), 131.8, 131.4 (quar, ^2J = 34 Hz, $ArCCF_3$), 129.9, 129.4, 128.8, 128.3, 126.6, 125.2, 124.6, 123.3, 123.1 (quar, ^1J = 271 Hz, CF_3), 122.7 (quar, ^1J = 271 Hz, CF_3), 73.7 (C^h), 70.8, 69.6, 58.7 (C^r), 48.0 (C^p), 44.3 (C^e), 37.4 (C^n), 28.7 (C^o). δ_F(377 MHz; $CDCl_3$) −62.5, −63.0. *m*/*z* (ES) 1133.3077 ($[M + Na]^+$ $C_{52}F_{12}H_{46}N_6NaO_8$ requires 1133.3078).

Axle 8. Azide **5** (50 mg, 0.15 mmol) and alkyne **2** (35 mg, 0.15 mmol) were dissolved in dry CH_2Cl_2 (3 mL) under an Ar (g) atmosphere. Then, $Cu(CH_3CN)_4BF_4$ (4.6 mg, 0.015 mmol), TBTA (7.8 mg, 0.015 mmol) and DIPEA (28 μL, 21 mg, 0.16 mmol) were added. The reaction was stirred at RT

for 18 h under an Ar (g) atmosphere. Then, the reaction was diluted to 10 mL, washed with 0.02 M EDTA in 1 M NH_3 (aq) solution (2 × 10 mL) and (1 × 10 mL) brine. The organic layer was dried ($MgSO_4$), filtered and solvent removed *in vacuo*. The crude material was purified by silica gel column chromatography (99 : 1 CH_2Cl_2/CH_3OH) to give the title compound as a transparent colourless film (75 mg, 88%). R_f = 0.33, 98 : 2 CH_2Cl_2/CH_3OH. ν_{max}/cm^{-1} (neat) 3300 (N–H), 3060 (C–H), 3030 (C–H), 2930 (C–H), 2860 (C–H), 1650 (C═O), 1540, 1450, 1380, 1280, 1170, 1130, 1050. δ_H(400 MHz; $CDCl_3$) 8.29 (2H, s, H^l), 8.01 (1H, s, H^k), 7.18–7.29 (12H, m, H^m, H^q & phenyl H), 4.62 (2H, s, H^r), 4.39 (2H, t, ^3J = 6.5 Hz, H^p), 4.27 (1H, t, ^3J = 7.2 Hz, H^t), 4.04 (^3J = 7.2 Hz, H^s), 3.47–3.51 (2H, app quar, H^n), 2.17–2.23 (2H, app quin, H^o). δ_C(100 MHz; $CDCl_3$) 164.8 (C═O), 145.4, 141.9, 136.1, 132.1 (quar, ^2J = 34 Hz, $ArCCF_3$), 128.4, 128.2, 127.5, 126.6, 125.0, 123.1, 122.9 (quar, ^1J = 272 Hz, CF_3), 73.9 (C^s), 64.3 (C^r), 51.0 (C^t), 48.1 (C^p), 37.4 (C^n), 29.4 (C^o). δ_F(377 MHz; $CDCl_3$) −62.8. *m*/*z* (ES) 599.1840 ([M + Na]$^+$ $C_{29}F_6H_{26}N_4NaO_2$ requires 599.1852).

Axle 9. Azide **5** (100 mg, 0.29 mmol) and alkyne **3** (87 mg, 0.29 mmol) were dissolved in dry CH_2Cl_2 (5 mL) under an Ar (g) atmosphere. Then, $Cu(CH_3CN)_4BF_4$ (9.1 mg, 0.029 mmol), TBTA (15.4 mg, 0.029 mmol) and DIPEA (60 μL, 42 mg, 0.32 mmol) were added. The reaction was stirred at RT for 48 h under an Ar (g) atmosphere. Then, the reaction was dilute to 10 mL, washed with 0.02 M EDTA in 1 M NH_3 (aq) solution (2 × 10 mL) and (1 × 15 mL) brine. The organic layer was dried ($MgSO_4$), filtered and solvent removed *in vacuo*. The crude material was purified by silica gel column chromatography (3 : 2 to 1 : 1 petrol 40–60/EtOAc) to give the title compound as a white solid (122 mg, 66%). R_f = 0.34, 98 : 2 CH_2Cl_2/CH_3OH. Mp 130–131 °C. ν_{max}/cm^{-1} (neat) 3340 (N–H), 3130 (C–H), 3090 (C–H), 1720 (ester C═O), 1650 (amide C═O), 1620, 1560, 1470, 1430, 1370, 1340, 1270, 1250, 1180, 1120. δ_H(400 MHz; $CDCl_3$) 8.47 (2H, s, H^s), 8.24 (2H, s, H^l), 8.07 (1H, s, H^t), 8.01 (1H, s, H^k), 7.87 (1H, s, H^q), 6.98 (1H, br s, H^m), 5.52 (2H, s, H^r), 4.54 (2H, t, ^3J = 6.5 Hz, H^p), 3.55–3.60 (2H, app quar, H^n), 2.29–2.35 (2H, app quin, H^o). δ_C(100 MHz; $CDCl_3$) 164.9, 163.8 (2 × C═O), 142.4, 136.0, 132.3 (quar, ^2J = 34 Hz, 2 × $ArCCF_3$), 131.7, 129.8, 127.3, 126.6, 125.2, 124.9, 122.8 (quar, ^1J = 272 Hz, CF_3), 122.8 (quar, ^1J = 272 Hz, CF_3, sic), 58.8 (C^r), 48.1 (C^p), 37.5 (C^n), 29.7 (C^o). δ_F(377 MHz; $CDCl_3$) −62.9, −63.0. *m*/*z* (ES) 659.0926 ([M + Na]$^+$ $C_{24}F_{12}H_{16}N_4NaO$ requires 659.0923).

Computational methodology

The Gaussian 09 program was used to conduct all density functional theory calculations.[18] In each case, geometry optimisations using the B3LYP/6-31G* model chemistry were undertaken,[19] with $CHCl_3$ solvent effects modelled using the default polarisable continuum model (and default solvent cavity parameters) as defined in Gaussian 09. To obtain reasonable starting structures, the structures were pre-optimised using a combination of molecular mechanics and semi-empirical PM6 methods. Several 'starting points' were considered for the optimisations, to minimise bias in the final structures.

Acknowledgements

We thank Lancaster University for financial support of this project. For a sample of alkyne **2** we thank Charles Gell (Lancaster University). For the recording of mass spectrometry data we thank the EPSRC UK National Mass Spectrometry Facility (NMSF) at Swansea University, UK (samples of **3** and **4**) and Dr David Rochester at Lancaster University, UK (samples of **5**, **6**, **7**, **8**, and **9**). For assistance in the recording of ^1H–^1H ROESY NMR spectra we thank Dr Geoff Akien (Lancaster University).

All underlying data for this paper are provided in the experimental section and the ESI.† Electronic copies of NMR spectra (including fid files) are available from DOI: 10.17635/lancaster/researchdata/132.

Notes and references

1 M. Xue, Y. Yang, X. Chi, X. Yan and F. Huang, *Chem. Rev.*, 2015, **115**, 7398–7501.
2 S. F. M. van Dongen, S. Cantekin, J. A. A. W. Elemans, A. E. Rowan and R. J. M. Nolte, *Chem. Soc. Rev.*, 2014, **43**, 99–122.
3 S. Erbas-Cakmak, D. A. Leigh, C. T. McTernan and A. L. Nussbaumer, *Chem. Rev.*, 2015, **115**, 10081–10206.
4 (*a*) C. Wu, P. R. Lecavalier, Y. X. Shen and H. W. Gibson, *Chem. Mater.*, 1991, **3**, 569; (*b*) J.-C. Chambron, V. Heitz and J.-P. Sauvage, *J. Chem. Soc., Chem. Commun.*, 1992, 1131–1133; (*c*) L. Hogg, D. A. Leigh, P. J. Lusby, A. Morelli, S. Parsons and J. K. Y. Wong, *Angew. Chem., Int. Ed.*, 2004, **43**, 1218–1221; (*d*) A. M. Fuller, D. A. Leigh, P. J. Lusby, I. D. H. Oswald, S. Parsons and D. B. Walker, *Angew. Chem., Int. Ed.*, 2004, **43**, 3914–3918; (*e*) V. Aucagne, K. D. Hänni, D. A. Leigh, P. J. Lusby and D. B. Walker, *J. Am. Chem. Soc.*, 2006, **128**, 2186–2187; (*f*) H. Lahlali, K. Jobe, M. Watkinson and S. M. Goldup, *Angew. Chem., Int. Ed.*, 2011, **50**, 4151–4155; (*g*) A. Noor, S. C. Moratti and J. D. Crowley, *Chem. Sci.*, 2014, **5**, 4283–4290; (*h*) J. E. Beves, B. A. Blight, C. J. Campbell, D. A. Leigh and R. T. McBurney, *Angew. Chem., Int. Ed.*, 2011, **50**, 9260–9327.
5 (*a*) P. R. Ashton, M. Grognuz, A. M. Z. Slawin, J. F. Stoddart and D. J. Williams, *Tetrahedron Lett.*, 1991, **32**, 6235–6238; (*b*) R. A. Bissell, E. Córdova, A. E. Kaifer and J. F. Stoddart, *Nature*, 1994, **369**, 133–137; (*c*) M. J. Gunter, N. Bampos, K. D. Johnstone and J. K. M. Sanders, *New J. Chem.*, 2001, **25**, 166–173; (*d*) G. Barin, A. Coskun, M. M. G. Fouda and J. F. Stoddart, *ChemPlusChem*, 2012, **77**, 159–185.
6 (*a*) F. Vögtle, M. Händel, S. Meier, S. Ottens-Hildebrandt, F. Ott and T. Schmidt, *Liebigs Ann.*, 1995, 739–743; (*b*) D. A. Leigh, A. Murphy, J. P. Smart and A. M. Z. Slawin, *Angew. Chem., Int. Ed.*, 1997, **36**, 728–732; (*c*) F. G. Gatti, D. A. Leigh, S. A. Nepogodiev, A. M. Z. Slawin, S. J. Teat and J. K. Wong, *J. Am. Chem. Soc.*, 2001, **123**, 5983–5989; (*d*) Y.-L. Huang, W.-C. Hung, Y.-H. Liu, S.-M. Peng and S.-H. Chiu, *Angew. Chem., Int. Ed.*, 2007, **46**, 6629–6633; (*e*) D. M. D'Souza, D. A. Leigh, L. Mottier, K. M. Mullen,

F. Paolucci, S. J. Teat and S. Zhang, *J. Am. Chem. Soc.*, 2010, **132**, 9465–9470; (*f*) A. Altieri, V. Aucagne, R. Carrillo, G. J. Clarkson, D. M. D'Souza, J. A. Dunnett, D. A. Leigh and K. M. Mullen, *Chem. Sci.*, 2011, **2**, 1922–1928; (*g*) R. Ahmed, A. Altieri, D. M. D'Souza, D. A. Leigh, K. M. Mullen, M. Papmeyer, A. M. Z. Slawin, J. K. Y. Wong and J. D. Wollins, *J. Am. Chem. Soc.*, 2011, **133**, 12304–12310; (*h*) A. Tron, P. J. Thornton, M. Rocher, H.-P. J. de Rouville, J.-P. Desvergne, B. Kauffmann, T. Buffeteau, D. Cavagnat, J. H. R. Tucker and N. D. McClenaghan, *Org. Lett.*, 2014, **16**, 1358–1361.

7 (*a*) P. R. Ashton, P. T. Glink, J. F. Stoddart, P. A. Tasker, A. J. P. White and D. J. Williams, *Chem. – Eur. J.*, 1996, **2**, 729–736; (*b*) H. Zheng, W. Zhou, J. Lv, X. Yin, Y. Li, H. Liu and Y. Li, *Chem. – Eur. J.*, 2009, **15**, 13253–13262; (*c*) V. Blanco, A. Carlone, K. D. Hänni, D. A. Leigh and B. Lewandowski, *Angew. Chem., Int. Ed.*, 2012, **51**, 5166–5169.

8 (*a*) G. M. Hübner, J. Gläser, C. Seel and F. Vögtle, *Angew. Chem., Int. Ed.*, 1999, **38**, 383–386; (*b*) C. A. Schalley, G. Silva, C. F. Nising and P. Linnartz, *Helv. Chim. Acta*, 2002, **85**, 1578–1596; (*c*) J. A. Wisner, P. D. Beer, M. G. B. Drew and M. R. Sambrook, *J. Am. Chem. Soc.*, 2002, **124**, 12469–12476; (*d*) E. Arunkumar, C. C. Forbes, B. C. Noll and B. D. Smith, *J. Am. Chem. Soc.*, 2005, **127**, 3288–3289; (*e*) L. M. Hancock, L. C. Gilday, S. Carvalho, P. J. Costa, V. Félix, C. J. Serpell, N. L. Kilah and P. D. Beer, *Chem. – Eur. J.*, 2010, **16**, 13082–13094.

9 A. Vidonne and D. Philp, *Tetrahedron*, 2008, **64**, 8464–8475.

10 T. Kosikova, N. I. Hassan, D. B. Cordes, A. M. Z. Slawin and D. Philp, *J. Am. Chem. Soc.*, 2015, **137**, 16074–16083.

11 A. Vidonne, T. Kosikova and D. Philp, *Chem. Sci.*, 2016, **7**, 2592–2603.

12 N. I. Hassan, V. del Amo, E. Calder and D. Philp, *Org. Lett.*, 2011, **13**, 458–461.

13 (*a*) C. W. Tornøe, C. Christensen and M. Meldal, *J. Org. Chem.*, 2002, **67**, 3057–3064; (*b*) V. V. Rostovtsev, L. G. Green, V. V. Fokin and K. B. Sharpless, *Angew. Chem., Int. Ed.*, 2002, **41**, 2596–2599; (*c*) J. E. Hein and V. V. Fokin, *Chem. Soc. Rev.*, 2010, **39**, 1302–1315.

14 C. N. Marrs and N. H. Evans, *Org. Biomol. Chem.*, 2015, **13**, 11021–11025.

15 N. H. Evans, C. E. Gell and M. J. G. Peach, *Org. Biomol. Chem.*, 2016, **14**, 7972–7981.

16 See ESI† for further NMR, IR and high resolution mass spectra of rotaxanes **6** & **7** and axles **8** & **9**.

17 See ESI† for coordinate data files from simulations.

18 M. J. Frisch, G. W. Trucks, H. B. Schlegel, G. E. Scuseria, M. A. Robb, J. R. Cheeseman, G. Scalmani, V. Barone, B. Mennucci, G. A. Petersson, H. Nakatsuji, M. Caricato, X. Li, H. P. Hratchian, A. F. Izmaylov, J. Bloino, G. Zheng, J. L. Sonnenberg, M. Hada, M. Ehara, K. Toyota, R. Fukuda, J. Hasegawa, M. Ishida, T. Nakajima, Y. Honda, O. Kitao, H. Nakai, T. Vreven, J. A. Montgomery, Jr., J. E. Peralta, F. Ogliaro, M. Bearpark, J. J. Heyd, E. Brothers, K. N. Kudin, V. N. Staroverov, R. Kobayashi, J. Normand, K. Raghavachari, A. Rendell, J. C. Burant, S. S. Iyengar, J. Tomasi, M. Cossi, N. Rega, J. M. Millam, M. Klene, J. E. Knox, J. B. Cross, V. Bakken, C. Adamo, J. Jaramillo, R. Gomperts, R. E. Stratmann, O. Yazyev, A. J. Austin, R. Cammi, C. Pomelli, J. W. Ochterski, R. L. Martin, K. Morokuma, V. G. Zakrzewski, G. A. Voth, P. Salvador, J. J. Dannenberg, S. Dapprich, A. D. Daniels, Ö. Farkas, J. B. Foresman, J. V. Ortiz, J. Cioslowski and D. J. Fox, *Gaussian 09, Revision E.01*, Gaussian, Inc., Wallingford Ct, 2009.

19 (*a*) A. D. Becke, *J. Chem. Phys.*, 1993, **98**, 5648–5652; (*b*) P. J. Stephens, F. J. Devlin, C. F. Chabalowski and M. J. Frisch, *J. Phys. Chem.*, 1994, **98**, 11623–11627; (*c*) A. D. Becke, *J. Chem. Phys.*, 1993, **98**, 1372–1377; (*d*) C. Lee, W. Yang and R. G. Parr, *Phys. Rev. B: Condens. Matter*, 1998, **37**, 785–789.

20 In the case of rotaxane **7** similar geometry optimisations were also run with the macrocycle starting over the ester functional group, but repeatedly the macrocycle would translate along the axle over the course of the optimisation, to one of the other "stations". This result is as would be expected as the ester group is unable to act as a hydrogen bond donor.

21 See ESI† for a full tabulated summary of energies and hydrogen bond distances in the simulated rotaxane structures.

22 As detailed in the ESI† for both rotaxanes, when the macrocycle resides at the amide "station", the axle N–H···O polyether hydrogen bond is significantly longer than the equivalent triazole C–H···O hydrogen bond when the macrocycle occupies the triazole "station". However, we hypothesise that this difference (which would favour macrocycle occupancy of the triazole "station") is outweighed by the interactions that favour occupancy of the amide "station" detailed in the main text.